

Data Report: UT-GOM2-1 Biostratigraphy Report Green Canyon Block 955, Gulf of Mexico¹

M. Purkey Phillips, The University of Texas, Institute for Geophysics, Austin, Texas, 78728

1. Abstract

This calcareous nannofossil biostratigraphy report includes the description and age estimation of 34 samples examined from 2 holes drilled during the 2017 UT-GOM2-1 Expedition in Green Canyon, Gulf of Mexico (GoM) – 22 samples from Hole H002, and 12 samples from H005.

2. Introduction

The UT-GOM2-1 Expedition in May, 2017 drilled two holes in Green Canyon Block 955 (GC 955) in the deepwater Gulf of Mexico: Hole GC 955 H002 (H002) and Hole GC 955 H005 (H005). 21 10 ft (3.05 m) pressure cores were attempted in, and near, the methane hydrate reservoir. In the first hole, H002, 1 of the 8 cores was recovered under pressure with 34% recovery of sediment (both pressurized and depressurized) (Flemings et al. 2018a; Thomas et al., 2020). In the second hole, H005, 12 of the 13 cores were recovered under pressure with 72% recovery of sediment. The remaining cores were recovered at atmospheric pressure (Flemings et al. 2018a; Thomas et al., 2020).

3. Methods and Materials

The biozonation applied to this age estimation is the Calcareous Nannofossil Plio- Pleistocene (CNPL) Zonation of Backman et al. (2012), which assigns Plio-Pleistocene biochronology to calcareous nannofossil assemblages from low to middle latitudes. This biozonation is further calibrated to the 2016 Geologic Time Scale of Ogg et al. (2016).

Semi-quantitative evaluations were conducted on all samples to identify age-diagnostic species/assemblages and estimate geologic age. All samples contain significant amounts of Cretaceous nannofossils that suggest reworking of sediments. These specimens are not

¹Purkey Phillips, M., 2020, Data Report: UT-GOM2-1 Biostratigraphy Report Green Canyon Block 955, Gulf of Mexico. In Proceedings of the UT-GOM2-1 Hydrate Pressure Coring Expedition: Austin, TX (University of Texas Institute for Geophysics, TX). 15 p.

Initial receipt: 10 May 2018

Acceptance: 1 June 2018

Publication: 30 Sept 2018

Amended: 9 December 2020

Corresponding Author: Marcie Purkey Phillips marciep@ig.utexas.edu

Volume: <https://dx.doi.org/10.2172/1646019>

<https://ig.utexas.edu/energy/genesis-of-methane-hydrate-in-coarse-grained-systems/expedition-ut-gom2-1/reports/>

considered part of the microfossil assemblage when making biostratigraphic age estimations; instead, they are considered part of the detrital sediment.

For more information regarding cores, lithostratigraphy, and core photos, the reader is referred to the following archives in the UT-GOM2-1 Data Directory (Flemings et al 2018b):

H002: http://www-udc.ig.utexas.edu/gom2/H002/6_Lithostratigraphy/

H005: http://www-udc.ig.utexas.edu/gom2/H005/6_Lithostratigraphy/

4. Results

4.1. UT-GOM2-1 Hole H002 Sample Descriptions

All samples examined from Hole H002 are estimated to be Late Calabrian to Early Ionian (late Middle Pleistocene). Sample UT-GOM2-1-H002-1CS-1_24-25cm, 409.6 mbsf, provides the first age- diagnostic data and is estimated to be no younger than 0.43 Ma. The lowermost sample, UT-GOM2-1-H002-8CS-5_27-28cm, 434.1mbsf, is estimated to be no older than 0.91 Ma. This estimated age range is assigned to the CNPL Zone 10. Samples in bold font indicate that age- diagnostic species were observed. See Figure 2 for detailed biostratigraphy.

H002-1CS-1_11-12cm, 409.46 mbsf: Calcareous nannofossil abundance is insufficient for biostratigraphic estimation.

H002-1CS-1_24-25cm, 409.59 mbsf: Primary age diagnostic species *Gephyrocapsa* “small” (<4µm) and “medium” (4-5.5µm) were observed in this sample. Based on this assemblage, geologic age is interpreted to be Calabrian/Ionian within Calcareous Nannofossil Zone CNPL10 (Calabrian/Ionian). Single specimens of each *Reticulofenestra asanoi* and *Emiliania huxleyi* were observed, and while they are both marker species, they are not age-diagnostic here. *R. asanoi* is probably in-situ, but is not age-diagnostic given its lack of abundance. *E. huxleyi* is interpreted as contamination. Specimens of *Sphenolithus abies* (Miocene-Pliocene) were observed and are also considered reworked.

H002-2CS-1_0-45cm, 412.84 mbsf: This sample is predominantly composed of reworked Cretaceous nannofossils. Presence and abundance of age diagnostic microfossils is insufficient.

H002-2CS-2_16-17cm, 413.01 mbsf: This sample contains virtually 100% reworked Cretaceous nannofossils indicating a strong influence of terrestrial runoff during this time of deposition. Presence and abundance of age diagnostic microfossils is insufficient. The preservation of Cretaceous specimens is noted to be very good.

H002-2CS-2_23cm, 413.07 mbsf: This sample contains virtually 100% reworked Cretaceous nannofossils. Presence and abundance of age diagnostic microfossils is insufficient.

H002-2CS-2_37-38cm, 413.21 mbsf: This sample contains virtually 100% reworked Cretaceous nannofossils. No microfossils from the estimated time of deposition were observed.

H002-2CS-3_59-60cm, 414.23 mbsf: This sample contains a greater diversity of Pleistocene

and modern nannofossils, but total abundance remains very low. Age diagnostic species *Gephyrocapsa* “small” and “medium” were observed, and the geologic age for this sample is estimated to be within Zone CNPL10.

H002-2CS-4_75-76cm, 415.39 mbsf: This sample is predominated by reworked Cretaceous specimens and low abundances of age diagnostic species including *Gephyrocapsa* “small” and “medium” supporting an age estimation within CNPL Zone 10.

H002-3CS-1_13-14cm, 415.57 mbsf: This sample contains virtually 100% reworked Cretaceous nannofossils. No microfossils from the estimated time of deposition were observed.

H002-5CS-1_75-76cm, 422.29 mbsf: This sample contains a greater diversity of Pleistocene and modern nannofossils, but total abundance remains very low. Age diagnostic species *Gephyrocapsa* “small” and “medium” were observed, and the geologic age for this sample is estimated to be within Zone CNPL10.

H002-6CS-1_10-11cm, 424.69 mbsf: This sample contains virtually 100% reworked Cretaceous nannofossils. No microfossils from the estimated time of deposition were observed.

H002-6CS-2_19-119cm, 424.78 mbsf: This sample contains virtually 100% reworked Cretaceous nannofossils. Presence and abundance of age diagnostic microfossils is insufficient.

H002-6CS-3_119-219cm, 425.78 mbsf: This sample contains virtually 100% reworked Cretaceous nannofossils. Preservation of Cretaceous specimens is good. Presence and abundance of age diagnostic microfossils is insufficient.

H002-6CS-4_16-17cm, 426.94 mbsf: This sample contains virtually 100% reworked Cretaceous nannofossils. No microfossils from the estimated time of deposition were observed. Large grains were notable in this sample, and all observed specimens were fragmented.

H002-6CS-5_8-9cm, 427.86 mbsf: This sample is predominantly composed of reworked Cretaceous nannofossils. It also contains low abundances of Pleistocene and modern nannofossils including a single specimen of *Gephyrocapsa* “large” (>5.5µm) that is likely in situ. The geologic age for this sample is estimated to be within Zone CNPL10. Ostracod shell fragments were also observed during examination. The single specimen of *E. huxleyi* is interpreted as contamination.

H002-7CS-1_6-72cm, 427.69 mbsf: This sample contains virtually 100% reworked Cretaceous nannofossils. Presence and abundance of age diagnostic microfossils is insufficient.

H002-8CS-2_57cm, 431.25 mbsf: This sample is predominantly composed of reworked Cretaceous nannofossils with very few Pleistocene nannofossils. Presence and abundance of

age diagnostic microfossils is insufficient.

H002-8CS-2_57-157cm, 432.25 mbsf: This sample is predominantly composed of reworked Cretaceous nannofossils with few specimens of *Gephyrocapsa* “small” observed, as well as a single specimen of age-diagnostic *Pseudoemiliana lacunosa*. This combination continues to support the Zone CNPL10 age assignment. While *P. lacunosa* is considered *in situ*, a single specimen should not be relied upon for precise age estimation. The single specimen of *E. huxleyi* is interpreted as contamination.

H002-8CS-3_157-235cm, 432.25 mbsf: This sample contains virtually 100% reworked Cretaceous nannofossils. Presence and abundance of age diagnostic microfossils is insufficient.

H002-8CS-4_5-6cm, 433.08 mbsf: This sample is predominantly composed of reworked Cretaceous nannofossils, and also contains moderate abundances of Pleistocene and modern nannofossils. Age diagnostic species of *Gephyrocapsa* “small” and “medium” were observed, which continue to support an estimated age within Zone CNPL10.

H002-8CS-4_33-34cm, 433.36 mbsf: This sample contains virtually 100% reworked Cretaceous nannofossils. No microfossils from the estimated time of deposition were observed.

H002-8CS-5_27-28cm, 434.1 mbsf: This sample is predominantly composed of reworked Cretaceous nannofossils, but also contains low abundances of *Gephyrocapsa* “small” and “medium”, which continue to support the estimated geologic age of Calabrian, Zone CNPL10. Multiple specimens of juvenile planktic forams were also observed in this sample.

4.2. UT-GOM2-1 Hole H005 Sample Descriptions

All samples examined from Hole H005 are also estimated to be Late Calabrian to Early Ionian, within the CNPL10 Zone. See Figure 4 for detailed biostratigraphy.

H005-1FB-3_163-184cm, 284.18 mbsf: This sample contains abundant age-diagnostic *Gephyrocapsa* “small” and “medium”, and *P. lacunosa*, whose concurrent ranges are estimated to be within CNPL Zone 10. Other Pliocene-Pleistocene age-diagnostic species were observed including *Ceratolithus cristatus*, *Discoaster challengeri*(?), *D. pentaradiatus*, and *Sphenolithus abies*. These four species; however, are considered reworked based on poor preservation and low abundance relative to the whole assemblage.

H005-3FB-2_0-17.5cm, 419.64-419.82 mbsf: This sample contains relatively abundant age-diagnostic *Gephyrocapsa* “small” and “medium” and *P. lacunosa*, whose concurrent ranges are estimated to be within CNPL Zone 10. Multiple specimens from the genera *Discoaster* and *Sphenolithus* were observed in this sample and are considered reworked based on poor preservation and low abundance relative to the whole assemblage.

H005-4FB-5_0-17.5cm_422.19-422.36 mbsf: This sample contains relatively abundant age-diagnostic *Gephyrocapsa* “small” and “medium” whose concurrent ranges are estimated to be within CNPL Zone 10. Multiple specimens from the genus *Discoaster* were observed in this sample and are considered reworked for the same reasons already listed.

H005-6FB-2_91.5-98.5cm_429.34-429.41mbsf: This sample contains age-diagnostic *Gephyrocapsa* “small” and “medium”, and *P. lacunosa*, whose concurrent ranges are estimated to be within CNPL Zone 10.

H005-9FB-1_15-16cm, 436.93 mbsf: This sample contains virtually 100% reworked Cretaceous nannofossils. Presence and abundance of age diagnostic microfossils is insufficient.

H005-9FB-2_34-35cm, 437.3 mbsf: This sample contains virtually 100% reworked Cretaceous nannofossils. No microfossils from the estimated time of deposition were observed.

H005-9FB-4_282-317cm, 439.36 mbsf: This sample contains virtually 100% reworked Cretaceous nannofossils. Presence and abundance of age diagnostic microfossils is insufficient.

H005-9FB-4_10-11, 439.46 mbsf: Specimens of the age-diagnostic *Gephyrocapsa* “small” were observed in very low abundances. Sufficient data is not available in this sample to estimate geologic age for this sample alone, but data from surrounding samples support a geologic age estimation within Zone CNPL10.

H005-11FB-1_0-27cm, 441.35-441.62 mbsf: This sample contains relatively abundant age-diagnostic *Gephyrocapsa* “small” and “medium”, and *P. lacunosa*, whose concurrent ranges are within CNPL Zone 10. One specimen of *Discoaster* was observed and is considered reworked.

H005-12FB-1_4-5cm, 444.44 mbsf: This sample contains virtually 100% reworked Cretaceous nannofossils. Specimens of the age-diagnostic *Gephyrocapsa* “small”, and *P. lacunosa* were observed in very low abundances. The observation of *P. lacunosa* was of a single specimen that was partially broken. Geologic age cannot be confidently estimated for this sample alone, but data from surrounding samples can support an estimated geologic age within Zone CNPL10.

H005-12FB-2_15-16cm, 444.55 mbsf: This sample contains virtually 100% reworked Cretaceous nannofossils. Presence and abundance of age diagnostic microfossils is insufficient.

H005-12FB-4_12-13, 445.28 mbsf: Very few specimens of age-diagnostic *Gephyrocapsa* “small” and “medium” were observed in low abundances, and an age-estimation within Zone CNPL10 is assigned. The single specimen of *E. huxleyi* is considered to be reworked.

5. SUMMARY/DISCUSSION

All samples examined from GOM2-1 holes H002 and H005 are estimated to be between 0.43 Ma and 0.91 Ma. This estimated age range straddles the Calabrian and Ionian stage boundary of the late Middle Pleistocene (Backman et al., 2012, Ogg et al., 2016). More specifically, all samples are estimated to be *within* the Calcareous Nannofossil Pleistocene (CNPL) Zone 10 as defined by the Biozonation of Miocene-Pleistocene calcareous nannofossils from low- to mid-latitudes (Backman et al., 2012).

The calcareous nannofossil assemblage that defines CNPL Zone 10, and the GOM 2-1 biostratigraphy samples, includes *Pseudoemiliana lacunosa* and *Gephyrocapsa* “medium” (4–5.5 μm). The last appearance datum (LAD), or extinction, of *P. lacunosa* defines the top of CNPL Zone 10 at 0.43 Ma. The shallowest sample in the GOM 2-1 sample interval contains *P. lacunosa*, and although it is impossible to say for sure without more samples whether this is the LAD, the working interpretation is that these samples likely are below the top of CNPL Zone 10 and the LAD of *P. lacunosa*. *Gephyrocapsa* “medium” predominates over *Gephyrocapsa* “small” (<4 μm) and “large” (>5.5 μm) through CNPL Zone 10 after an earlier interval of absence in CNPL Zone 9. The top of the absence of *Gephyrocapsa* “medium” – when they re-enter the record – marks the top of CNPL Zone 9 and the base of CNPL Zone 10 at 1.06 Ma. Straddling the boundary of CNPL Zones 9 and 10 is a short-lived biological event defined as the “common occurrence” of *Reticulofenestra asanoi* from 1.14 – 0.91 Ma. This event was not observed in the GOM 2-1 samples and, therefore, the sample interval is interpreted to be younger than 0.91 Ma.

The overall biostratigraphic interpretation is bolstered by integrating the data from both holes (only 12 m apart); and integration is supported by Thomas’ et al. (2020) correlation of hydrate-bearing layers between holes H002 and H005, as well as Hole H001 that was drilled in 2009 (Figure 5).

The accuracy of this interpretation is moderate for several reasons including 1) limited recovery and limited sampling, 2) coarse grain size of sample material, and 3) the sample interval, which is limited to the targeted channel levee. Accuracy would be improved by 1) collecting samples from clay-rich or mud intervals whenever possible, and 2) collecting additional samples above and below the channel-levee target interval to increase probability of intersecting finer-grained lithofacies and additional biological events to improve and confirm the working age estimation.

Core recovery was significantly more successful in hole H005 (85%) than in H002 (34%) (Thomas et al., 2020). Cored material included both hydrate-bearing pressure cores and conventionalized pressure cores. Biostratigraphy samples were collected from both types of cored material, including failed pressure cores. In spite of better core recovery, in-situ microfossil assemblages were more robust in hole H002 (Figure 1 & 2), but more age-diagnostic species were identified in hole H005 (Figure 3 & 4), further supporting the value of data integration.

UT-GOM2-1 cores were recovered from only the target hydrate reservoir, which is a

Pleistocene channel-levee complex composed of sandy silt and clayey silt lithofacies (Flemings et al., 2020; Santra et al., 2020). One exception is the uppermost core 1FB in hole H005 (Figure 4), which is from the overburden and is the most fine-grained lithology encountered in either hole described as silty clay (Flemings et al., 2020; Meazell et al., 2020;). The two main reservoir lithofacies described by Meazell et al (2020) are interpreted to be a product of turbidity flows. Each couplet of sandy silt and clayey silt records a single turbidity current flow sourced by an overspilling turbidity current that flowed down the channel axis and deposited on the levees. Flemings et al. (2020) and Phillips et al. (2020) further recognized that the clayey silt samples have a broad size distribution with considerable variability between samples, some of which have sand-silt laminae within and are thus more coarse-grained. The silty clay observed from the overburden core is interpreted to be formed most likely by hemipelagic sedimentation or possible distal turbidity currents.

There is an indirect relationship between grain-size and microfossil abundance. Most biostratigraphy samples examined from holes H002 and H005 were from silty intervals, and microfossil abundance is, therefore, relatively low (Figures 2 & 4). Since most microfossils, specifically calcareous nannofossils, are clay-sized (<25 μm), energy regimes that are strong enough to deposit silts and sands (e.g. turbidites and submarine channels) are typically too strong to retain and preserve calcareous nannofossils. Nannofossils would, however, be more abundant in the fine-grained distal flow of a turbidite as well as other fine-grained depositional facies. The fine-grained tail of the turbidity current could also deposit reworked nannofossils. Despite the turbiditic influence on these samples, the microfossils are still reliable, age-diagnostic tools.

Of the 34 samples examined for biostratigraphy, only 14 contained age-diagnostic assemblages. Of those 14 samples, 11 were silty yet contained age-diagnostic assemblages that were relatively reliable based on good preservation and moderate abundance. Three samples were exceptional with lithologies more conducive to microfossil preservation, particularly sample H005-1FB-3_163-184cm at 284.18 mbsf - the uppermost sample of the interval – which was taken from the hemipelagic overburden above the hydrate reservoir and is described as a silty clay lithofacies. H005-1FB is the only core between both holes with this lithologic description (Flemings et al., 2020; Meazell et al., 2020). The other two samples with higher quality microfossil assemblages are H002-5CS-1_75-76cm, 422.29 mbsf and H002-8CS-4_5-6cm, 433.08 mbsf, which are both near the base of the sample interval.

In addition to the Pleistocene microfossil assemblage, a relatively abundant and diverse reworked Cretaceous nannofossil assemblage was observed in every sample. This reworked assemblage is preserved in the channel-levee lithology as part of the detritus eroded and transported from the continent. Therefore, the reworked Cretaceous nannofossil assemblage is considered a component of the lithology rather than the microfossil assemblage and may be capable of indicating provenance.

6. Acknowledgements

This work and the UT-GOM2-1 Hydrate Pressure Coring Expedition was funded by the Department of Energy Award DE-FE0023919, which is advised by the United States Geological Survey (USGS) and the Bureau of Ocean Energy Management (BOEM).

This report was prepared as an account of work sponsored by an agency of the United States Government. Neither the United States Government nor any agency thereof, nor any of their employees, makes any warranty, express or implied, or assumes any legal liability or responsibility for the accuracy, completeness, or usefulness of any information, apparatus, product, or process disclosed, or represents that its use would not infringe on privately owned rights. Reference herein to any specific commercial product, process, or service by trade name, trademark, manufacturer, or otherwise does not necessarily constitute or imply its endorsement, recommendation, or favoring by the United States Government or any agency thereof. The views and opinions of authors expressed herein do not necessarily state or reflect those of the United States Government or any agency thereof.

7. References

- Backman, J., Raffi, I., Rio, D., Fornaciari, E., Pälke, 2012. Biozonation and biochronology of Miocene through Pleistocene calcareous nannofossils from low and middle latitudes. *Newsletters on Stratigraphy*, 45 (3), 221-244.
- Flemings, P. B., S. C. Phillips, R. Boswell, T. S. Collett, A. E. Cook, T. Dong, and M. Frye, et al., 2020, Pressure coring a Gulf of Mexico deep-water turbidite gas hydrate reservoir: Initial results from The University of Texas-Gulf of Mexico 2-1 (UT-GOM2-1) Hydrate Pressure Coring Expedition: *AAPG Bulletin*, v. 104, no. 9, p. 1847-1876, <https://doi.org/10.1306/05212019052>.
- Flemings, P.B., Phillips, S.C, Collett, T., Cook, A., Boswell, R., and the UT-GOM2-1 Expedition Scientists, 2018a. UT-GOM2-1 Hydrate Pressure Coring Expedition Summary. In Flemings, P.B., Phillips, S.C, Collett, T., Cook, A., Boswell, R., and the UT-GOM2-1 Expedition Scientists, *Proceedings of the UT-GOM2-1 Hydrate Pressure Coring Expedition*, Austin, TX (University of Texas Institute for Geophysics, TX). <http://dx.doi.org/10.2172/1647223>.
- Flemings, P.B., Phillips, S.C, Collett, T., Cook, A., Boswell, R., and the UT-GOM2-1 Expedition Scientists, 2018b, UT-GOM2-1 Hydrate Pressure Coring Expedition Data Directory, <http://www-udc.ig.utexas.edu/gom2/>.
- Meazell, K., P. Flemings, M. Santra, and J. E. Johnson, 2020, Sedimentology and stratigraphy of a deep-water gas hydrate reservoir in the northern Gulf of Mexico: *AAPG Bulletin*, v. 104, no. 9, p. 1945–1969, <https://doi.org/10.1306/05212019027>.
- Ogg, J., Ogg, G., Gradstein, F., 2016. *A Concise Geologic Time Scale 2016*. Elsevier B.V., ISBN978-0-444-63771-0.

Phillips, S.C., P.B., ME. Holland, P.J. Schultheiss, W.F. Waite, J. Jang, E.G. Petrou, and Hammon, 2020. High concentration methane hydrate in a silt reservoir from the deep-water Gulf of Mexico: AAPG Bulletin, v. 104, no. 9, p. 1971-1995, [https://doi.org/ 10.1306/01062018280](https://doi.org/10.1306/01062018280)

Santra, M., P. B. Flemings, E. Scott, and P. K. Meazell, 2020, Evolution of gas hydrate-bearing deep-water channel-levee system in abyssal Gulf of Mexico: Levee growth and deformation: AAPG Bulletin, v. 104, no. 9, p. 1921-1944, <https://doi.org/10.1306/04251918177>.

Thomas, C., S. C. Phillips, P. B. Flemings, M. Santra, H. Hammon, T. S. Collett, and A. Cook, et al., 2020, Pressure-coring operations during The University of Texas-Gulf of Mexico 2-1 (UT-GOM2-1) Hydrate Pressure Coring Expedition in Green Canyon Block 955, northern Gulf of Mexico: AAPG Bulletin, v. 104, no. 9, p. 1877–1901, <https://doi.org/10.1306/02262019036>.

8. Figures

Figure 1. H002 Calcareous Nannofossil Distribution. A copy of the figure can be found at http://www-udc.ig.utexas.edu/gom2/H002/6_Lithostratigraphy/Biostratigraphy/

API:
 AREA: Green Canyon
 BLOCK:
 GCS (LEASE):
 WELL NUMBER: H002
 OPERATOR: University of Texas, Jackson School of Geosciences
 PALEONTOLOGIST: Marie Purkey Phillips
 FIRE SAMPLE: 409.49 mof

UTGOM2-1_H002 Nannofossil Distribution

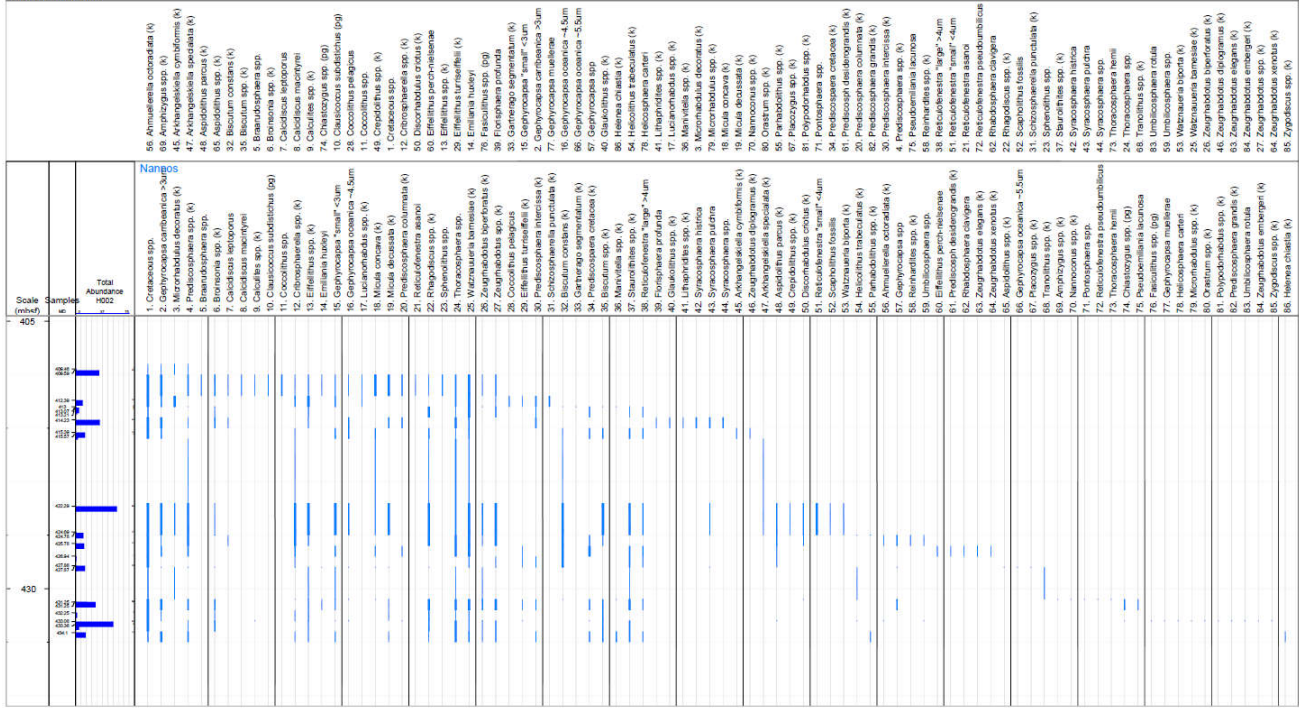


Figure 2. Chart H002 Biostratigraphy Chart. A copy of the figure can be found at http://www-udc.ig.utexas.edu/gom2/H002/6_Lithostratigraphy/Biostratigraphy/

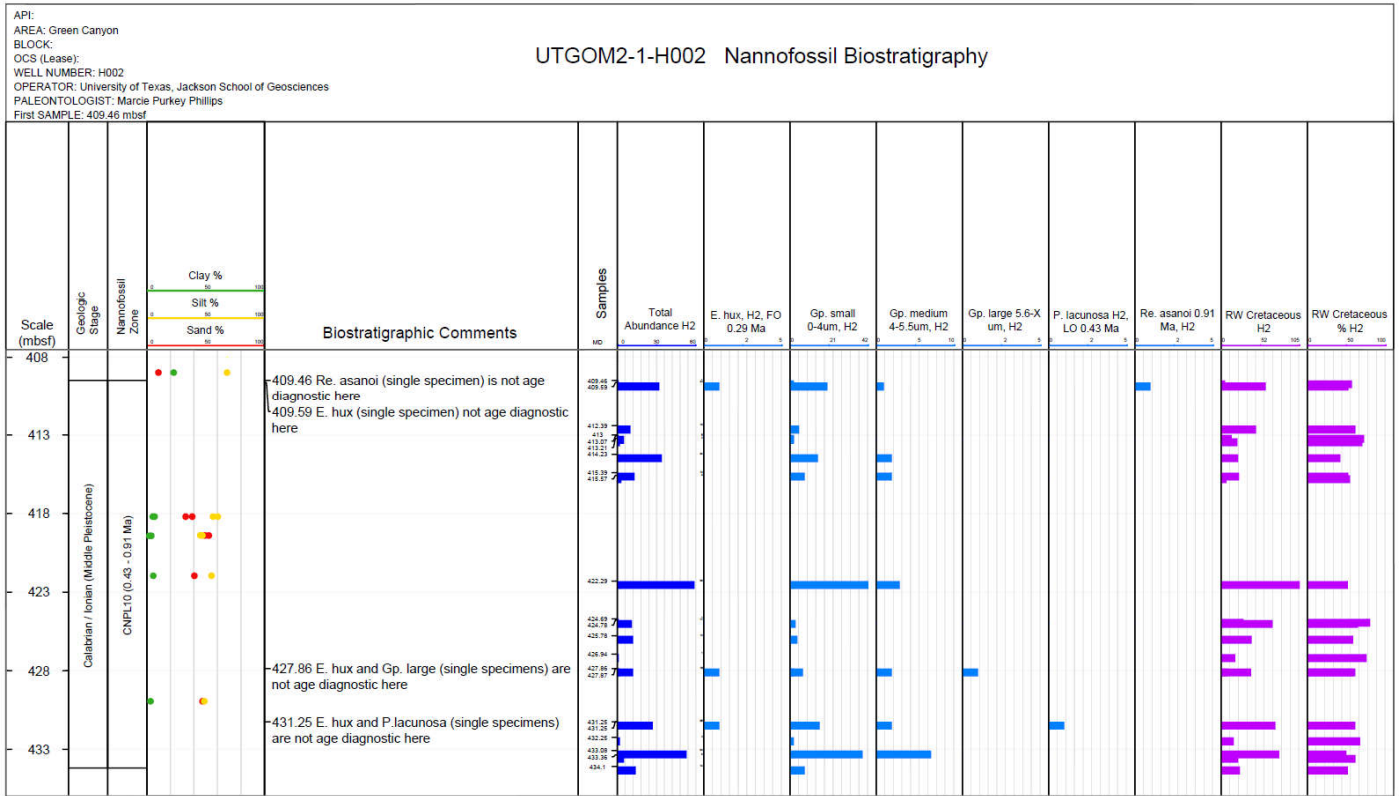


Figure 3. H005 Calcareous Nannofossil Distribution. A copy of the figure can be found at http://www-udc.ig.utexas.edu/gom2/H005/6_Lithostratigraphy/Biostratigraphy/.

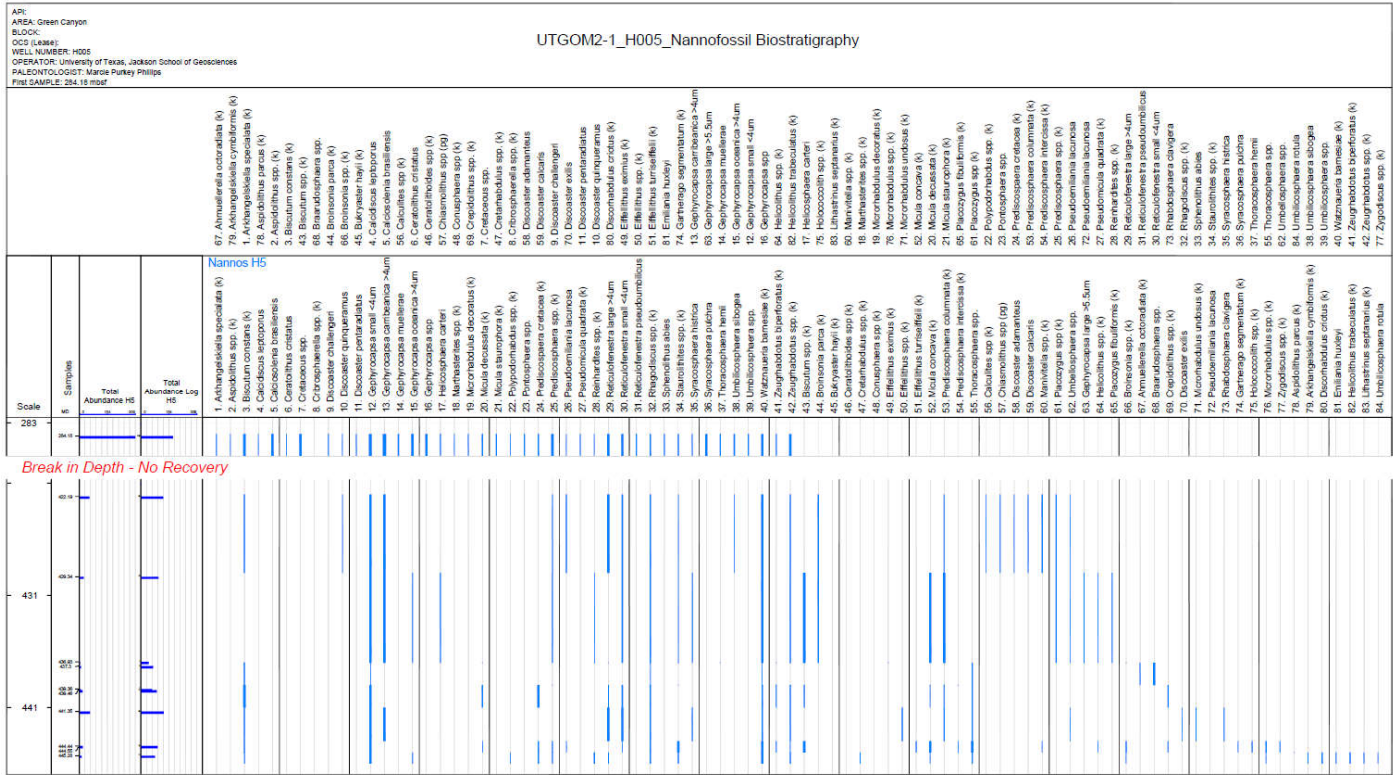


Figure 4. Chart H005 Biostratigraphy Chart. A copy of the figure can be found at http://www-udc.ig.utexas.edu/gom2/H005/6_Lithostratigraphy/Biostratigraphy/.

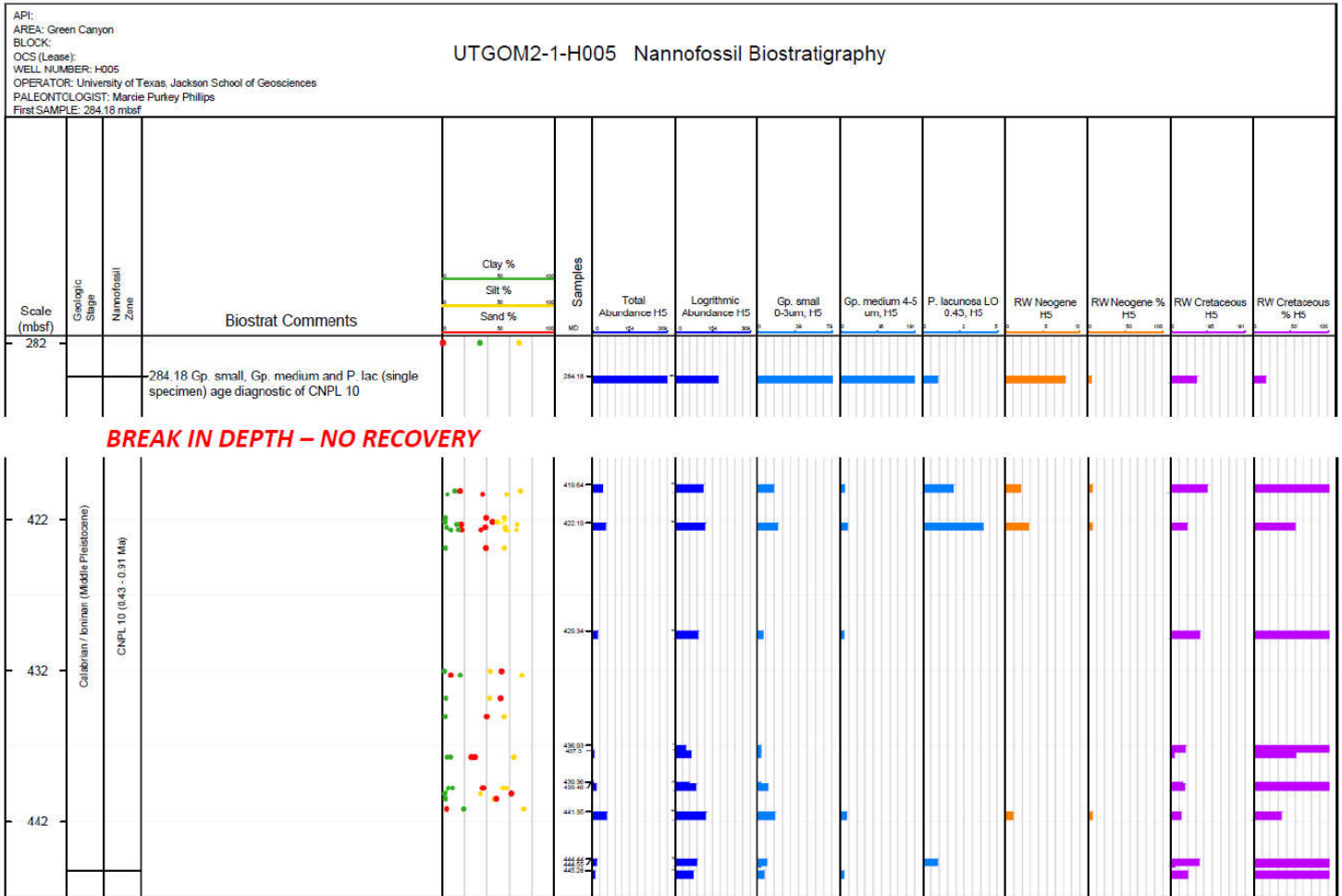
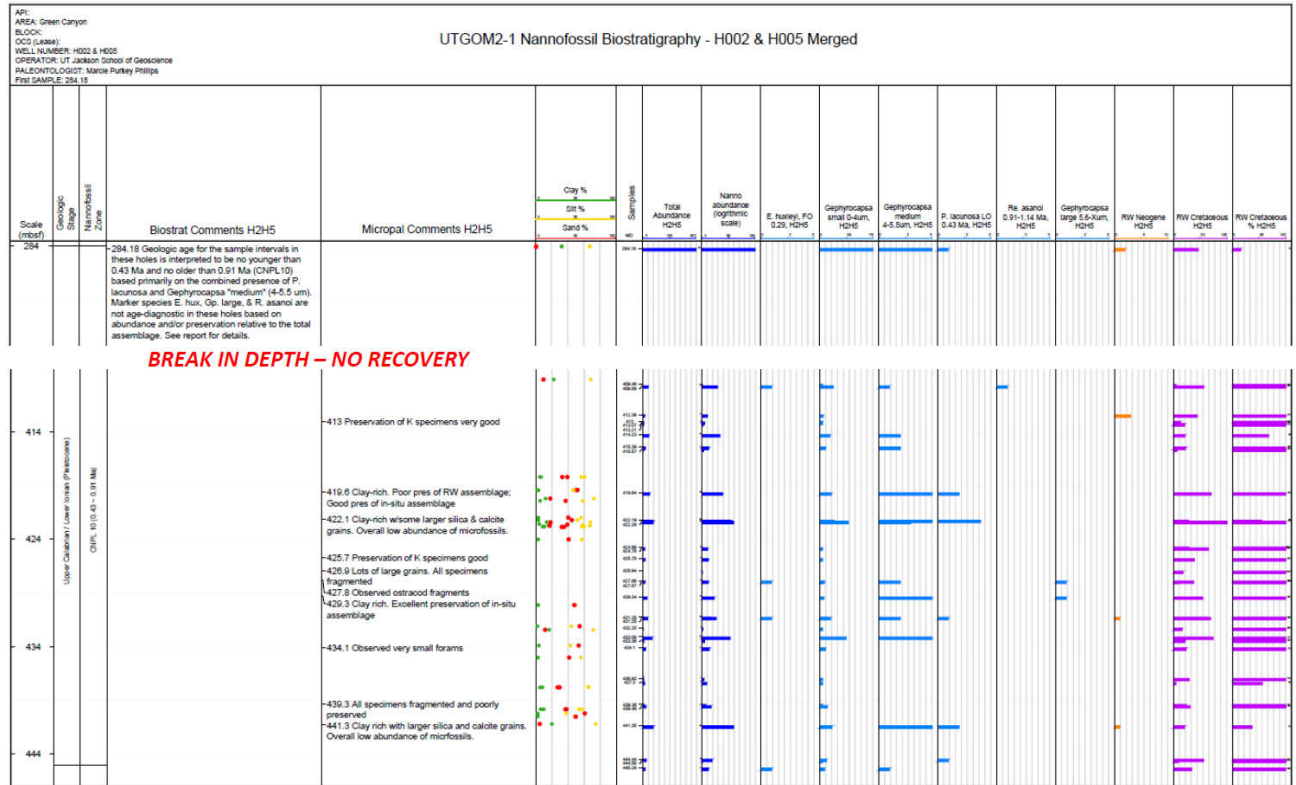


Figure 5. Chart H002 and H005 Integrated Biostratigraphy Chart. A copy of the figure can be found at http://www-udc.ig.utexas.edu/gom2/H005/6_Lithostratigraphy/Biostratigraphy/.



9. Tables

Table 1. H002 Data spreadsheet. A copy of the spreadsheet can be found at http://www-udc.ig.utexas.edu/gom2/H002/6_Lithostratigraphy/Biostratigraphy/.

Expedition	Hole	Core	Section	Interval Top (cm)	Interval Base (cm)	Depth Top (mbsf)	Depth Base (mbsf)	Geologic Stage (Ogg et al., 2016)	Nannofossil Zone (Bakken et al., 2012)	Forams	Total Sum	Total c/f = Ng	Total K	Total Pg	Total K	Total Pg	Comments
UTGOM2-1	H002	1	11	12	409.46	409.47											
UTGOM2-1	H002	1	24	25	409.59	409.6											
UTGOM2-1	H002	1	0	45	412.39	412.84											
UTGOM2-1	H002	2	16	17	413	413.01											
UTGOM2-1	H002	2	23	23	413.07	413.07											
UTGOM2-1	H002	2	37	38	413.21	413.22											
UTGOM2-1	H002	3	59	60	414.23	414.24											
UTGOM2-1	H002	3	75	76	415.39	415.4											
UTGOM2-1	H002	3	13	14	415.57	415.58											
UTGOM2-1	H002	3	75	76	422.29	422.3											
UTGOM2-1	H002	3	110	111	424.69	424.7											
UTGOM2-1	H002	3	119	119	424.78	425.78											
UTGOM2-1	H002	3	119	219	425.78	426.78											
UTGOM2-1	H002	3	16	17	426.94	426.95											
UTGOM2-1	H002	3	8	9	427.86	427.87											
UTGOM2-1	H002	3	72	72	427.69	428.35											
UTGOM2-1	H002	3	57	57	431.25	431.25											
UTGOM2-1	H002	3	57	157	431.25	432.25											
UTGOM2-1	H002	3	157	235	432.25	433.03											
UTGOM2-1	H002	3	5	6	433.08	433.09											
UTGOM2-1	H002	3	34	34	433.36	433.37											
UTGOM2-1	H002	3	27	28	434.1	434.2											

Table 2. H005 Data spreadsheet. A copy of the spreadsheet can be found at http://www-udc.ig.utexas.edu/gom2/H005/6_Lithostratigraphy/Biostratigraphy/.

Expedition	Hole	Core	Section	Interval Top (cm)	Interval Base (cm)	Depth Top (mbsf)	Depth Base (mbsf)	Geologic Stage (Ogg et al., 2016)	Nannofossil Zone (Bakken et al., 2012)	Forams	Total Sum	Total c/f = Ng	Total K	Total Pg	Total K	Total Pg	Comments
UTGOM2-1	H005	11B	3	163.0	184.0	284.18	284.39										
UTGOM2-1	H005	9FB	2	0.0	17.5	419.64	419.82										
UTGOM2-1	H005	4FB	5	0.0	17.5	422.19	422.36										
UTGOM2-1	H005	6FB	2	91.5	98.5	429.34	429.41										
UTGOM2-1	H005	9FB	1	15.0	16.0	436.93	436.94										
UTGOM2-1	H005	9FB	2	34.0	35.0	437.3	437.4										
UTGOM2-1	H005	9FB	4	282.0	317.0	438.36	438.99										
UTGOM2-1	H005	9FB	4	10.0	11.0	439.46	439.47										
UTGOM2-1	H005	11FB	1	0.0	27.0	441.35	441.62										
UTGOM2-1	H005	12FB	1	4.0	5.0	444.44	444.45										
UTGOM2-1	H005	12FB	2	15.0	16.0	444.55	444.56										
UTGOM2-1	H005	12FB	3	12.0	13.0	445.28	445.29										